



LAWRENCE
LIVERMORE
NATIONAL
LABORATORY

Surface water processes in the Indonesian Throughflow as documented by a high-resolution coral ($\Delta^{14}\text{C}$) record

S. J. Fallon, T. P. Guilderson

April 28, 2008

Journal of Geophysical Research (Oceans)

Disclaimer

This document was prepared as an account of work sponsored by an agency of the United States government. Neither the United States government nor Lawrence Livermore National Security, LLC, nor any of their employees makes any warranty, expressed or implied, or assumes any legal liability or responsibility for the accuracy, completeness, or usefulness of any information, apparatus, product, or process disclosed, or represents that its use would not infringe privately owned rights. Reference herein to any specific commercial product, process, or service by trade name, trademark, manufacturer, or otherwise does not necessarily constitute or imply its endorsement, recommendation, or favoring by the United States government or Lawrence Livermore National Security, LLC. The views and opinions of authors expressed herein do not necessarily state or reflect those of the United States government or Lawrence Livermore National Security, LLC, and shall not be used for advertising or product endorsement purposes.

1
2
3
4 Surface water processes in the Indonesian Throughflow as documented by a
5 high-resolution coral $\Delta^{14}\text{C}$ record
6
7

8
9 Stewart J. Fallon^{1*}, Thomas P. Guilderson^{1,2}
10

11
12 1. Center for Accelerator Mass Spectrometry, Lawrence Livermore National Laboratory,
13 Livermore, California, USA.
14

15 2. Department of Ocean Sciences, and Institute of Marine Sciences, University of
16 California, Santa Cruz, California, USA.
17

18 *Now at Research School of Earth Sciences, The Australian National University,
19 Canberra, Australia
20

Abstract

To explore the seasonal to decadal variability in surface water masses that contribute to the Indonesian Throughflow we have generated a 115-year bi-monthly coral-based radiocarbon time-series from a coral in the Makassar Straits. In the pre-bomb (pre-1955) era from 1890 to 1954, the radiocarbon time series occasionally displays a small seasonal signal (10-15‰). After 1954 the radiocarbon record increases rapidly, in response to the increased atmospheric ^{14}C content caused by nuclear weapons testing. From 1957 to 1986 the record displays clear seasonal variability from 15 to 60‰ and the post-bomb peak (163 per mil) occurred in 1974. The seasonal cycle of radiocarbon can be attributed to variations of surface waters passing through South Makassar Strait. Southern Makassar is under the influence of the Northwest Monsoon, which is responsible for the high Austral summer radiocarbon (North Pacific waters) and the Southeast Monsoon that flushes back a mixture of low (South Pacific and upwelling altered) radiocarbon water from the Banda Sea. The coral record also shows a significant ^{14}C peak in 1955 due to bomb ^{14}C water advected into this region in the form of CaCO_3 particles (this implies that the particles were advected intact and then become entrapped in the coral skeleton - is this what we really mean? Wouldn't even fine particles settle out over the inferred transit time from Bikini to MAK?) or water particles with dissolved labeled CO_2 produced during fallout from the Castle tests in 1954.

Introduction

The Indonesian throughflow (ITF) is thought to play an important role in global thermohaline circulation and influence global climate by funneling Pacific Warm Pool

water into the Indian Ocean [Broecker, 1991; Gordon, 1986; Gordon and Piola, 1983; Hirst and Godfrey, 1993]. Observations suggest the ITF is composed of North Pacific subtropical and thermocline waters that flow through Makassar Strait [Ffield and Gordon, 1992; Fine, 1985; Gordon and Fine, 1996; Ilahude and Gordon, 1996]. At the southern end of Makassar Strait water flows through Lombok Strait to the south and eastward into the Banda Sea ending up in the Indian Ocean (Figure 1). An additional component of deep South Pacific water enters Eastern Indonesia and mixes in the Banda Sea [Ffield and Gordon, 1992; Hautala, et al., 1996]. The flow of waters through the ITF is highly variable, estimates of -2 to 20 Sv have been reported [Godfrey, 1996; Gordon and Fine, 1996; Lukas, et al., 1996; Myers, 1996; Potemra, et al., 1997]. The atmospheric pressure gradient between the Pacific and Indian Ocean which results in a dynamic height difference between the two oceans is the main driving force for the ITF [Wyrski, 1987]. The dynamic height difference is greatest during the Southeast Monsoon (Southern Hemisphere winter) resulting in the strongest flow [Gordon, et al., 1999; Murray and Arief, 1988; Wyrski, 1987]. During the Northwest Monsoon (Southern Hemisphere summer) the gradient lessens, thereby weakening the throughflow [Gordon, et al., 1999; Murray and Arief, 1988; Wyrski, 1987]. Additionally, the NW monsoon decreases the surface salinity due to a large influx of freshwater via rainfall and runoff.

Throughflow variability and flow volume is correlated with the state of ENSO [Gordon, et al., 1999]. During La Niña events an increase in the sea surface height in the Western Pacific Warm Pool region results in an increase in the dynamic height gradient with the Indian Ocean and a corresponding increase in the throughflow volume, with the converse occurring during El Niño events [Gordon, et al., 1999]. Vertical

69 mixing influences the composition of the ITF. Heat and freshwater are transported down
70 toward the thermocline and cool water mixes upward potentially influencing the
71 atmosphere-ocean heat flux [*Ffield and Gordon*, 1992; 1996]. The ITF results in a
72 significant export of heat and freshwater from the tropical Pacific into the Indian Ocean
73 and may influence atmosphere-ocean coupling, tropical SST patterns and the Asian
74 Monsoon [*Schneider*, 1998]. One way to examine the sources and variability of the
75 throughflow is to use a water mass tracer. The radiocarbon ($\Delta^{14}\text{C}$) content of waters can
76 be used to track ocean currents, vertical mixing, and air-sea CO_2 exchange [*Druffel*, 1985;
77 *Druffel*, 1987; *Guilderson, et al.*, 2000a; *Guilderson, et al.*, 2000b; *Guilderson, et al.*,
78 1998; *Moore, et al.*, 1997].

79 Measurements of sub-annual samples from coral skeletal material provide a proxy
80 time-series record of the $\Delta^{14}\text{C}$ of the dissolved inorganic carbon (DIC) of the surrounding
81 seawater [*Druffel*, 1981; *Druffel and Suess*, 1983; *Guilderson, et al.*, 1998; *Moore, et al.*,
82 1997]. In this paper, we present the radiocarbon content in roughly bi-monthly samples
83 from a coral in the Makassar Strait to study the processes governing water mass evolution
84 in the Indonesian Seas over time scales long enough to study the linkage between
85 processes in the Indonesian Seas and decadal modulation of ENSO, Asian Monsoon and
86 global climate.

87 ***Methods***

88 **Coral**

89
90 A 2.3m core was drilled from a *Porites lutea* coral off Langkai Island ($5^{\circ}02' \text{ S}$,
91 $119^{\circ}04' \text{ E}$; Figure 1) [*Moore, et al.*, 1997]. The core was cut to a thickness of 9mm
92 [*Moore, et al.*, 1997] and sonicated in distilled water. This study builds on the original

Langkai $\Delta^{14}\text{C}$ dataset that spanned 1970-1985 published by Moore, et al. [1997]. The samples reported here were re-milled from the same coral core as Moore, et al. [1997] along a main growth axis. Samples were milled sequentially in 1.8 mm increments using a manual low-speed mill with a 2mm diameter mill bit, corresponding to ~6-8 samples per year. ^{14}C sample splits (8-10 mg) were reacted in individual chambers (BD Vacutainer), evacuated, heated and acidified with orthophosphoric acid at 90°C [Guilderson, et al., 2000b; Guilderson, et al., 1998]. The CO_2 was purified, trapped, and converted to graphite using an iron catalyst following a method similar to that described by Vogel, et al., [1987]. The graphite targets were analyzed at the Center for Accelerator Mass Spectrometry, Lawrence Livermore National Laboratory. The ^{14}C results are reported as age-corrected $\Delta^{14}\text{C}$ (‰) as defined by Stuiver and Polach [1977] and include $\delta^{13}\text{C}$ correction for isotope fractionation, and a blank subtraction based on ^{14}C -free calcite. Radiocarbon accuracy and precision is $\pm 3.5\%$ (1σ) based on long-term statistics of secondary standards. A coral tertiary standard was analyzed with the unknown coral samples with a resulting total precision of $\pm 0.75\%$ (1σ) ($n=88$) (Figure 2). This result is consistent with the analytical uncertainty of the measurements. Additional sample splits (~100 μg) were analyzed on a Finnigan MAT 252 with a Kiel carbonate device using 105% H_3PO_4 at 90°C. Stable isotope data are reported relative to the Vienna Pee Dee Belemnite (V-PDB) with an average analytical precision of $\pm 0.03\%$.

An initial age-model and time series was constructed using the seasonal variability in coral $\delta^{13}\text{C}$. In some tropical reef locations the coral $\delta^{13}\text{C}$ is modulated by seasonal light cycles. Higher light levels are associated with more positive $\delta^{13}\text{C}$ whereas lower light levels are associated with more negative $\delta^{13}\text{C}$ [Fairbanks and Dodge, 1979;

116 *McConnaughey, 1989*]. For this project we are assuming that the coral $\delta^{13}\text{C}$ primarily
117 tracks variability in solar insolation and that $\delta^{13}\text{C}$ inflection points are interpreted as
118 markings of seasonal change. In this part of Indonesia, the maximum cloudiness and
119 maximum rainfall occur in February/March. To generate the primary time series we
120 pinned the minimum $\delta^{13}\text{C}$ to February of each year, and linearly interpolated the data
121 between marker points. We then used the seasonal cycle of $\delta^{18}\text{O}$, which is influenced by
122 water temperature and fresh water to fine-tune the time series [references: Michael
123 Moore's dissertation and the Charles et al., *Mar Geol* paper]. Coral $\delta^{18}\text{O}$ is negatively
124 correlated with water temperature, the summer $\delta^{18}\text{O}$ coral signal is heavily influenced by
125 rainfall and runoff, so we matched the coral $\delta^{18}\text{O}$ maxima to the winter SST minimum
126 from the GOSTA SST atlas [*Bottomley, et al., 1990*]. With our sampling resolution this
127 results in a time series that is precise to ± 2 months.

129 ***Results and Discussion***

130 The coral $\Delta^{14}\text{C}$ time series spans 1870 to 1990. The pre-bomb interval (1870-
131 1950) has an average $\Delta^{14}\text{C}$ value of -56.5‰ (Figure 3a) and does not exhibit a consistent
132 seasonal cycle. During this period there is a very weak secular decrease of $\sim 8\text{‰}$ (based
133 on a least squares fit). $\Delta^{14}\text{C}$ begins to slowly increase in January 1954 with a more rapid
134 increase in February 1955 (Figure 3). The first large, sustained peak above the prebomb
135 average value occurs in July 1955 (Figure 3), where values jump from -50‰ in January
136 1955 to -7.2‰ in July 1955. After this early peak, $\Delta^{14}\text{C}$ values decrease until October
137 1957 after which time they begin to slowly rise until after 1962 when they rise rapidly to
138 a post-bomb max of 163.3‰ in Jan. 1974 (Figure 3). The peak occurs at approximately

the same time as that in the northern hemisphere subtropics [*Guilderson, et al.*, 2000b] which implies a lateral mixing processes dominated by N. Pacific source waters. The pre to post bomb $\Delta^{14}\text{C}$ amplitude is 220‰. A strong $\Delta^{14}\text{C}$ seasonal signal occurs after 1957 with varying amplitude ranging from 15 to 65‰ (Figure 3b).

From 1957 to 1986 the record displays clear seasonal variability of 15 to 65‰. The seasonal cycle of radiocarbon can be attributed to variations in the ^{14}C of surface waters passing the coral in Makassar Strait. During the NW Monsoon (Jan. – Mar.) *Gordon, et al.* [2003] showed that low salinity surface waters from the Java Sea (due to high rainfall/runoff) can lower the temperature and salinity of water entering the Indian Ocean (Figure 4A). The NW monsoon wind pushes the low salinity surface water from the Java Sea into South Makassar and possibly even northward into the strait itself. This low salinity surface water also flows into the Banda Sea and ultimately the Indian Ocean. During the opposite season (Southeast Monsoon) the winds push the Banda Sea surface waters westward back toward South Makassar and perhaps even slightly northward due to the northward flowing meridional winds [*Gordon, et al.*, 2003]. Sea surface temperature and salinity records indicate the Banda Sea is an area of intense vertical mixing (upwelling), resulting in lower surface seawater ^{14}C content [*Cresswell and Luick*, 2001; *Ffield and Gordon*, 1996]. We attribute the coral seasonal radiocarbon signal to this seesaw effect of the monsoon.

The strong seasonal $\Delta^{14}\text{C}$ cycle observed in this coral displays high radiocarbon values during the austral summer (Feb.). The seasonal maximum $\Delta^{14}\text{C}$ values are associated with the maximum eastward component of the Java Sea Zonal wind and the

fresh/warm water signal preserved by the coral $\delta^{18}\text{O}$ record [Moore, *et al.*, 1997; Charles *et al.*, 2000]. At first this seems to fit nicely with the Gordon *et al.* (2003) idea of fresh warm water from the Java Sea during the NW monsoon being advected into the southern end of Makassar Strait. However, the high coral radiocarbon values are more indicative of unmodified North Pacific source waters entering Makassar Strait and flowing southward past the Langkai coral site and not waters arriving via the Java Sea. We suggest that there may be northward flowing low salinity water from the Java Sea into Makassar Strait (as per Gordon *et al.*, 2003) but it is tightly constrained along the western boundary of the Makassar Strait. (Figure 4A).

Seasonally low radiocarbon values occur during the austral winter when the zonal wind component is at its westward maximum, the meridional component is northward, and the coral $\delta^{18}\text{O}$ indicates cool/dry conditions (Figure 5)[Moore, *et al.*, 1997]. We infer that the low radiocarbon waters are sourced from the Banda Sea (East Indonesian Seas) (Figure 4B), which has inputs of South Pacific water (lower in $\Delta^{14}\text{C}$ than N. Pacific water) modified by mixing with upwelled, subsurface, lower- ^{14}C water. During the NW monsoon the Banda Sea acts as a reservoir, filling up and deepening the thermocline by ~55m [Cresswell and Luick, 2001; Field and Gordon, 1996]. The shoaling of the thermocline during the austral winter SE monsoon and the extensive upwelling in the Banda Sea can account for the low ^{14}C surface waters [Wyrki, 1961]. These data imply that surface water flows from the Banda Sea back into the southern confines of Makassar Strait during the SE monsoon. (Figure 4B). This supports the ideas of the “flush back” of Banda Sea waters of Gordon, *et al.* (2003). Therefore our coral record observes the movement of high radiocarbon surface waters through Makassar Strait during the

warm/wet NW monsoon and the “flush back” of low- ^{14}C “upwelling altered” surface waters from the Banda Sea during the cooler SE monsoon. Our interpretation is slightly different to the one proposed by *Moore, et al.* (1997). They argue that the seasonal cycle is due to seasonal radiocarbon variability in the open waters of the Pacific as inferred from a 4-year ^{14}C -coral series at Guam. The “seasonal” cycle at Guam is not very clear or consistent and does not fit the timing of warm water temperature and high $\Delta^{14}\text{C}$ (See Figure 3 in [*Moore, et al.*, 1997]).

Early Bomb Peak

This coral $\Delta^{14}\text{C}$ record exhibits an interesting set of radiocarbon peaks commencing in February 1955. The coral/seawater $\Delta^{14}\text{C}$ DIC increases by 40‰ from –50‰ to –10‰ in 3 months with high values continuing until Nov. 1955 (Figure 6). This is a tremendous change and a significant source of ^{14}C is needed to alter the seawater $\Delta^{14}\text{C}$ DIC. During the first part of 1954 the United States of America conducted a series of thermonuclear weapons tests at Bikini Atoll (11° 35N, 165° 23E). This started with the 15 MT “Bravo” test on March 1, 1954, followed by tests on Mar. 27 (11 MT), Apr. 26 (6.9MT) and May 5 (13.5 MT) [*Yang, et al.*, 2000]. A significant labeling of waters around the Marshall Islands and to the west must have take place either by gas phase CO_2 exchange or particulate fallout (adsorbed onto CaCO_3 particles). The large rise observed in this coral suggests that fallout and not air/sea CO_2 exchange must be the source of the ^{14}C signature in the surface waters observed at Langkai. General open ocean air-sea CO_2 exchange is too slow to account for the rapid rise in coral/seawater $\Delta^{14}\text{C}$.

The general westward flow of the North Equatorial Current (NEC) must have brought this labeled water toward the Philippines and into the ITF via the Mindanao

Current (Figure 1). Seawater ^{90}Sr measurements in the Philippines, show high levels (850 dpm/ 100L of seawater) by the spring of 1955 suggesting that weapons test labeled water was there in high concentration [Miyake and Saruhashi, 1958]. Since the waters of the Philippines and the Mindanao Current are sourced from the NEC it follows that this labeled water entered the ITF and flowed past the coral site at Langkai. In an elegant study, Toggweiler and Trumbore [1985] reported elevated ^{90}Sr measurements in coral skeletal material from Cocos Island (12.5 S, 97E Indian Ocean) band counted to the year 1955. Konishi, et al., [1982] observed a 40‰ increase in $\Delta^{14}\text{C}$ in a coral from Okinawa from 1955 to 1956. All of these observations suggest a 1 yr. transit time for waters originating in the Marshall Islands to reach the bottom of Makassar Strait.

Another interesting feature of this part of the record is that the high $\Delta^{14}\text{C}$ values occur during May-Nov. 1955 (the SE monsoon) and not during the NW monsoon as the post 1958 record (Figures 2,5). The subsequent year, 1956, has 2 cycles peaking in Apr. and Nov. (Figure 6). The time period 1954 to 1957 was a moderately strong La Niña, suggesting that the surface wind and sea level pressure field during the La Niña event (more North Pacific water) and not the Indonesian monsoon was the dominant surface flow during this time period. Since there was no testing in 1955 the two peaks in 1956 indicate that some type of “storage” or new input of labeled (high $\Delta^{14}\text{C}$) water occurred. The peaks in 1957 could be due to further testing in 1956 (Figure 6).

Pre-bomb era

The Langkai pre-bomb (1870-1950) $\Delta^{14}\text{C}$ record exhibits an overall secular decrease of ~8‰. Although consistent with the dilution of atmospheric ^{14}C by the combustion of ^{14}C -free fossil fuel carbon (the so called Suess effect) and its subsequent

transfer into the surface ocean, we do not believe that the time-series is only influenced by the Suess Effect. $\Delta^{14}\text{C}$ values between 1870-1890 are $\sim 5\text{‰}$ higher than the 1891-1905 average (Figure 7A), thus most of the decrease occurs prior to a significant decrease in atmospheric $\Delta^{14}\text{CO}_2$, particularly when considering the decadal time constant of air-sea isotopic equilibrium. We hypothesize that the reason for the decrease is a change in either the proportion of Banda Sea water ‘back flushing’ the Southern Makassar Strait, or an increase in the upwelling in the Banda Sea that are coincident with an overall decrease of higher $\Delta^{14}\text{C}$ waters sourced from the Northern hemisphere subtropics.

Superimposed on this shift are interannual $\Delta^{14}\text{C}$ oscillations that are consistent with the redistribution of Pacific surface waters driven by ENSO. The coral $\delta^{18}\text{O}$ record (not shown) suggests that 1876-1878 was a significant drought on the same order of magnitude as the 1982/1983 El Niño drought. This time period corresponds to the low $\Delta^{14}\text{C}$ seen in Figure 7A (arrow). This low period is surrounded by higher $\Delta^{14}\text{C}$ in 1874/75 and 1879/80, which may be due to stronger La Niña conditions bringing more N. Pacific water through the ITF and less dilution by Banda Sea water during the S.H. winter. In the instrumental record, stronger than average El Niño events often are terminated by stronger than average La Niña events. In the context of the weaker pre-bomb spatial surface ocean $\Delta^{14}\text{C}$ gradients, only strong events are likely to provide a consistent signal in our surface water reconstruction. The pre-bomb interval is dominated by an inconsistent seasonal $\Delta^{14}\text{C}$ cycle, although some years do appear to follow the $\delta^{18}\text{O}$ cyclicity similar to the post-bomb era (data not shown). The lack of a distinct seasonal

cycle is due to the lower spatial $\Delta^{14}\text{C}$ gradient between the water masses prior to nuclear weapons testing.

To examine the coral record in relation to ENSO frequency fluctuations of ITF water we applied a (2.6-8 yr.) band-pass filter to the coral $\Delta^{14}\text{C}$ data and to the Southern Oscillation Index (Figure 7B,C). The comparison implies a gross coupling between the two records (Figure 7B). Higher $\Delta^{14}\text{C}$ occurs during positive SOI events, which is analogous to the S.E. Monsoon and greater throughflow (more North Pacific water) (Figure 7B). Also seen are low $\Delta^{14}\text{C}$ and negative SOI (El Niño events), analogous to the NW Monsoon or less throughflow (less North Pacific water) (Figure 7B). We remind the reader that the amplitude of surface $\Delta^{14}\text{C}$ is not a direct proxy for the strength and intensity of the ENSO event, particularly during the post-bomb interval [Guilderson *et al.*, 1998]. The Makassar record is a reflection of changes in the $\Delta^{14}\text{C}$ signature of waters that are sourced into the ITF. These dynamic processes are imprinted upon an evolving $\Delta^{14}\text{C}$ background where, in the post-bomb period, the bomb- ^{14}C transient is being mixed into and with waters with less ^{14}C .

The two records are coherent during the 1889 and 1905 ENSO events; the strong events of 1878 also appear in the $\Delta^{14}\text{C}$ record (Figure 7B). Throughout the record there are mismatches, especially in the post-bomb (1950-1990) period, that may be due to the variable nature of ENSO and a temporally varying $\Delta^{14}\text{C}$ pattern. We also cannot discount the effect of the monsoon winds and their interactions, both positive and negative with ENSO, causing different surface circulation in southern Makassar resulting in misfits between the two datasets. Thus the $\Delta^{14}\text{C}$ time series reinforces that the Indonesian Seas' surface water is a complex interaction between seasonally varying local winds, and

externally forced variability that incorporates both ENSO and the Asian Monsoon. This complex interaction excludes of the common and simplistic ENSO-centric interpretation of surface ocean ^{14}C time-series. Additional and strategically located coral-based records in concert with data-model comparisons [eg., Rodgers et al., 2004] will provide a strong tool to explore the seasonal to decadal controls on the mixing and dynamics of the Indonesesian Seas.

Implications for ITF Surface Circulation

The surface coral radiocarbon record presented here documents a complicated surface water circulation pattern of North Pacific waters arriving during the SH summer NW Monsoon and a flush back of mixed (S. Pacific and upwelling altered) waters from the Banda Sea during the SE Monsoon. Recent studies have shown that the main flow of the ITF is at depths of 200-400m and that surface flow can act independently of the subsurface flow [Gordon, et al., 2003]. Although not a pancea to place all variability in a dynamical context, El Niño and La Niña events do manifest themselves as surface water mass variations that are often times discernible in the $\Delta^{14}\text{C}$ time-series. A potential measurement of surface water transit speeds in the West Pacific is provided by the arrival of a ^{14}C signature resulting from early weapons tests (in 1955-57) that documents a transit time from the Marshall Islands through the ITF of approximately one-year.

Acknowledgements

We thank Chris Charles and Michael Moore for access to the Langkai coral samples and, at the time, unpublished data. Paula Zermeño, Dot Kurdyla and Sam Heller

assisted in the graphite lab pressing graphite targets. Special thanks to Dave Mucciarone and Rob Dunbar for allowing us to analyze stable isotopes at Stanford University. This work was performed under the auspices of the U.S. Department of Energy by Lawrence Livermore National Laboratory under Contract No. DE-AC52-07NA27344. Funding for this project was supplied by UC/LLNL LDRD 01-ERI-009 to T.G. Data will be archived at WDC-A, Boulder CO.

References:

- Bottomley, M., C. K. Folland, J. Hsiung, R. E. Newell, and D. E. Parker (1990), Global ocean surface temperature atlas "GOSTA", 20 pp, Meteorological Office, Bracknell, UK and the Department of Earth, Atmospheric and Planetary Sciences, Massachusetts Institute of Technology, Cambridge, MA, USA.
- Broecker, W. S. (1991), The Great Ocean Conveyor, *Oceanography*, 4, 79-89.
- Cresswell, G., and J. L. Luick (2001), Current measurements in the Halmahera Sea, *Journal of Geophysical Research*, 106, 13945-13952.
- Charles, C. D., K. Cobb, M. D. Moore, and R. G. Fairbanks (2003), Monsoon-tropical ocean interaction in a network of coral records spanning the 20th century, *Mar. Geology*, 201, 207-222.
- Druffel, E. M. (1981), Radiocarbon in annual coral rings from the eastern tropical Pacific Ocean, *Geophysical Research Letters*, 8, 59-62.
- Druffel, E. M., and H. E. Suess (1983), On the radiocarbon record in banded corals: Exchange parameters and net transport of $^{14}\text{CO}_2$ between atmosphere and surface ocean, *Journal of Geophysical Research*, 88, 1271-1280.
- Druffel, E. R. (1985), Detection of El Niño and decade time scale variations of sea surface temperature from banded coral records: implications for the carbon dioxide cycle., in *The Carbon Cycle and Atmospheric CO₂: Natural Variations Archean to Present.*, edited by E. Sundquist and W. S. Broecker, pp. 111-123, American Geophysical Monograph.
- Druffel, E. R. M. (1987), Bomb radiocarbon in the Pacific: Annual and seasonal timescale variations, *Journal of Marine Chemistry*, 45, 667-698.
- Fairbanks, R. G., and R. E. Dodge (1979), Annual periodicity of the $^{18}\text{O}/^{16}\text{O}$ and $^{13}\text{C}/^{12}\text{C}$ ratios in the coral *Monastrea annularis*, *Geochim. Cosmochim. Acta*, Vol. 43, 1009-1020.
- Ffield, A., and A. L. Gordon (1992), Vertical mixing in the Indonesian thermocline, *J. Phys. Oceanogr.*, 22, 184-195.
- Ffield, A., and A. L. Gordon (1996), Tidal mixing signatures in the Indonesian Seas, *Journal of Physical Oceanography*, 26, 1924-1937.

338 Fine, R. (1985), Direct evidence of using tritium data for throughflow from the Pacific
 339 into the Indian Ocean, *Nature*, 315, 478-480.
 340 Godfrey, J. S. (1996), The effect of the Indonesian throughflow on ocean circulation and
 341 heat exchange with the atmosphere: A review, *J. Geophys. Res.*, 101, 12,217-212,237.
 342 Gordon, A. (1986), Inter-ocean exchange of thermocline water, *Journal of Geophysical*
 343 *Research*, 91, 5037-5046.
 344 Gordon, A., and A. R. Piola (1983), Atlantic Ocean upper layer salinity budget, *Journal*
 345 *of Physical Oceanography*, 13, 1293-1300.
 346 Gordon, A. L., and R. Fine (1996), Pathways of water between the Pacific and Indian
 347 oceans in the Indonesian seas, *Nature*, 379, 146-149.
 348 Gordon, A. L., R. D. Susanto, and A. Ffield (1999), Throughflow within Makassar Strait,
 349 *Geophysical Research Letters*, 26, 3325-3328.
 350 Gordon, A. L., R. D. Susanto, and K. Vranes (2003), Cool Indonesian throughflow as a
 351 consequence of restricted surface layer flow, *Nature*, 425, 824-828.
 352 Guilderson, T. P., K. Caldeira, and P. B. Duffy (2000a), Radiocarbon as a diagnostic
 353 tracer in ocean and carbon cycle modeling, *Global Biochem. Cycles*, 14, 887-902.
 354 Guilderson, T. P., D. P. Schrag, E. Goddard, M. Kashgarian, G. M. Wellington, and B. K.
 355 Linsley (2000b), Southwest subtropical Pacific surface radiocarbon in a high-resolution
 356 coral record, *Radiocarbon*, 42, 249-256.
 357 Guilderson, T. P., D. P. Schrag, M. Kashgarian, and J. Southon (1998), Radiocarbon
 358 variability in the western equatorial Pacific inferred from a high-resolution coral record
 359 from Nauru Island, *J. Geophys. Res.*, 103, 24,641-24650.
 360 Hautala, S., J. Reid, and N. Bray (1996), The distribution and mixing of Pacific water
 361 masses in the Indonesian Seas, *J. Geophys. Res.*, 101, 12,375-312,389.
 362 Hirst, A. C., and J. S. Godfrey (1993), The role of Indonesian throughflow in a global
 363 ocean GCM, *Journal of Physical Oceanography*, 23.
 364 Ilahude, A. G., and A. L. Gordon (1996), Thermocline stratification within the Indonesian
 365 Seas, *J. Geophys. Res.*, 101, 12,401-412,409.
 366 Lukas, R., T. Yamagata, and J. P. McCreary (1996), Pacific low-latitude western
 367 boundary currents and the Indonesian throughflow, *J. Geophys. Res.*, 101, 12,209-
 368 212,216.
 369 McConnaughey, T. (1989), ^{13}C and ^{18}O isotopic disequilibrium in biological carbonates:
 370 II. In vitro simulation of kinetic isotope effects, *Geochem. Cosmochim. Acta*, 53, 163-
 371 171.
 372 Miyake, Y., and K. Saruhashi (1958), Distribution of man-made radioactivity in the
 373 North Pacific through summer 1955, *J. Mar. Res.*, 17, 383-?
 374 Moore, M. D., D. P. Schrag, and M. Kashgarian (1997), Coral radiocarbon constraints on
 375 the source of the Indonesian throughflow, *Journal of Geophysical Research*, 102, 12,359-
 376 312,365.
 377 Murray, S. P., and D. Arief (1988), Throughflow into the Indian Ocean through the
 378 Lombok Strait. January 1985-January 1986, *Nature*, 333, 444-447.
 379 Myers, G. (1996), Variation of Indonesian throughflow and the El Nino Southern
 380 Oscillation, *J. Geophys. Res.*, 101, 12,255-212,263.
 381 Potemra, J., R. Lukas, and G. Mitchum (1997), Large-scale estimation of transport from
 382 the Pacific to the Indian Ocean, *J. Geophys. Res.*, 102, 27,795-727,812.

Rodgers K. B., O. Aumont, G. Madec, C. Menkes, B. Blanke, P. Monfray, J. C. Orr, D. P. Schrag (2004), Radiocarbon as a thermocline proxy for the eastern equatorial Pacific, *Geophys. Res. Lett.*, 31, L14314, doi:10.1029/2004GL019764.

Schneider, N. (1998), The Indonesian throughflow and the global climate system, *J. Climate*, 11, 676-689.

Stuiver, M., and H. A. Polach (1977), Discussion: Reporting of ^{14}C Data, *Radiocarbon*, 19, 355-363.

Stuiver, M., P. J. Reimer, and T. F. Braziunas (1998), High-Precision radiocarbon age calibration for terrestrial and marine samples, *Radiocarbon*, 40, 1127-1151.

Toggweiler, J. R., and S. Trumbore (1985), Bomb-test ^{90}Sr in Pacific and Indian Ocean surface water as recorded by banded corals, *Earth and Planetary Science Letters*, 74, 306-314.

Vogel, J. S., J. R. Southon, and D. E. Nelson (1987), Catalyst and binder effects in the use of filamentous graphite for AMS, *Nuclear Instruments and Methods in Physics Research*, B29, 50-56.

Wyrtki, K. (1961), Physical oceanography of the Southeast Asian waters, 195 pp, Scripps Institute of Oceanography.

Wyrtki, K. (1987), Indonesian throughflow and associated pressure gradient, *J. Geophys. Res.*, 92, 12,941-12,946.

Yang, X., R. North, and C. Romney (2000), CMR Nuclear Explosion Database (Rev. 3), CMR Technical Report.

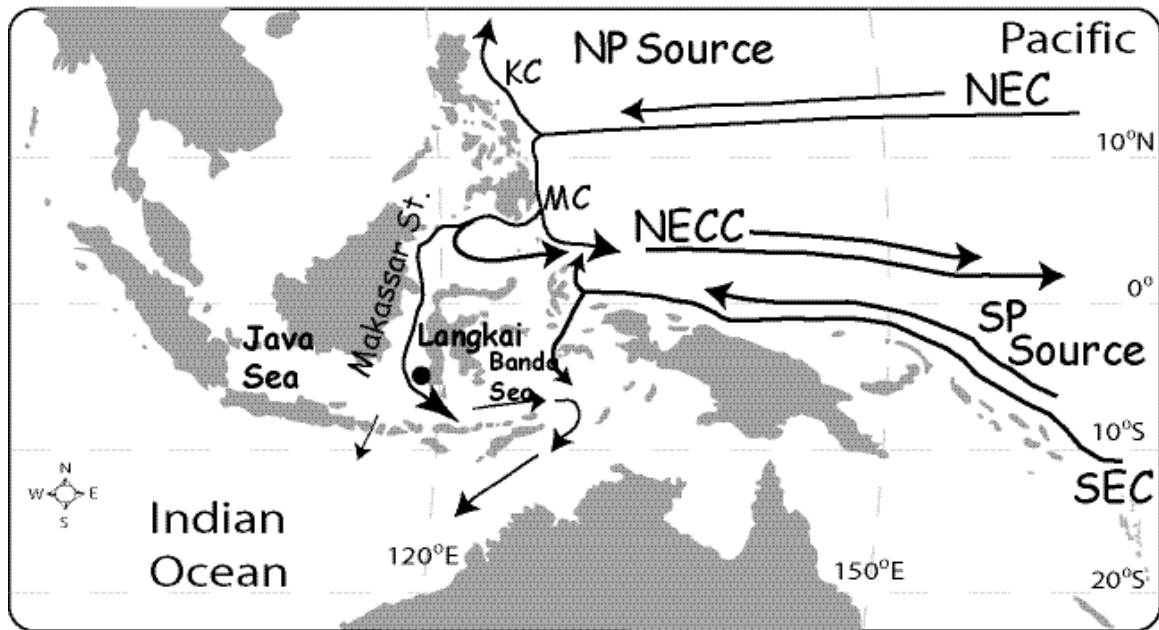


Figure 1. Indonesian archipelago showing sample site Langkai, and major currents and water sources in the area.

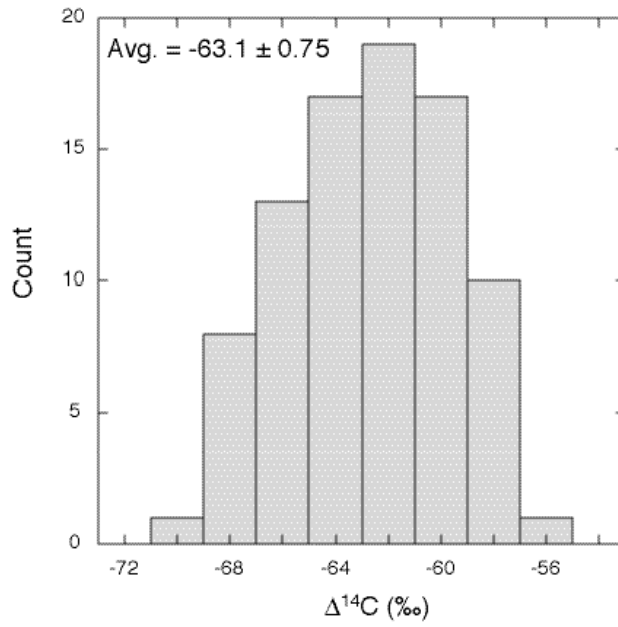


Figure 2. Histogram of secondary coral standard UCI-2, the average value is -63.1 ± 0.75 ‰, n=88.

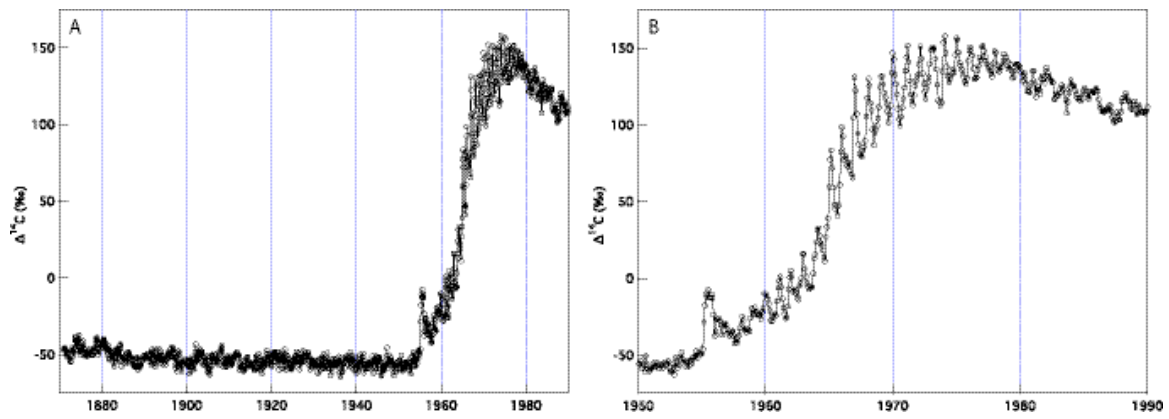


Figure 3. Coral radiocarbon record from Langkai. A) Time series spans the time frame 1870-1990. B). Close up of time frame 1950-1990.

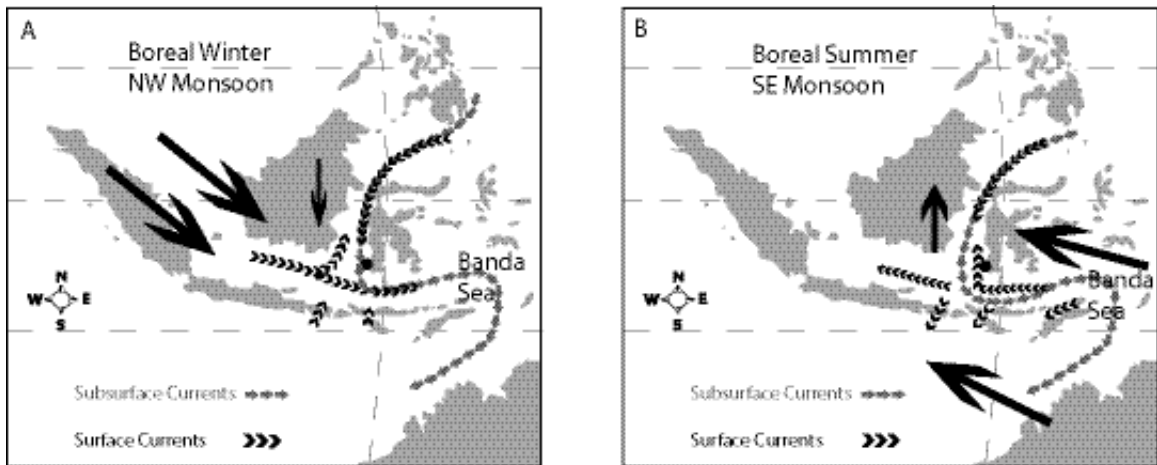


Figure 4. Indonesian Sea surface currents during Northwest Monsoon (A) and Southeast Monsoon (B). Winds are shown in large arrows. Diagram adapted from Gordon et al. [2003].

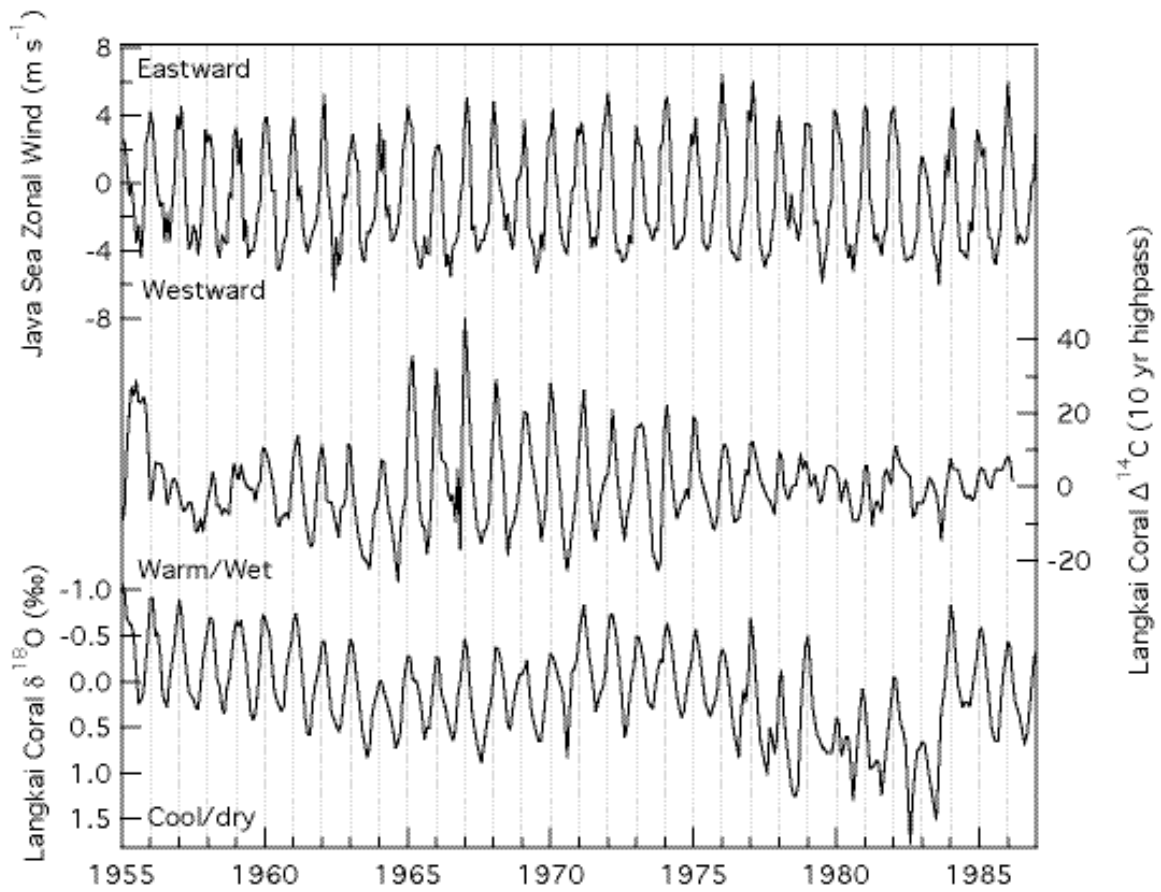


Figure 5. A sub-section of the Langkai coral $\Delta^{14}\text{C}$ time series after filtering with a high-pass filter (Tukey-cosine with a half-amplitude at 10 years) in relation to the coral $\delta^{18}\text{O}$ and the Java Sea (110° - 118° E; 4° - 7° S) Zonal wind speed.

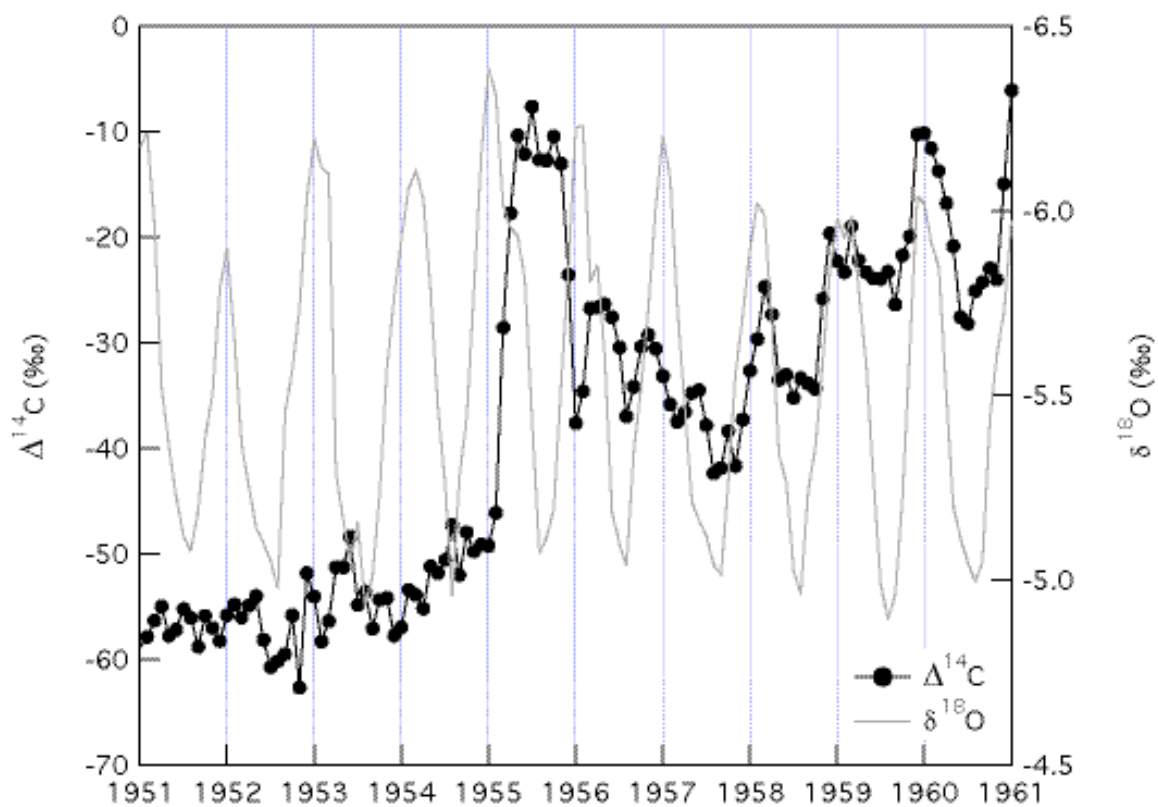


Figure 6. Close-up of mid-1950s bomb- ^{14}C induced coral/seawater DIC $\Delta^{14}\text{C}$ increase. Superimposed is the coral $\delta^{18}\text{O}$ to show seasonality.

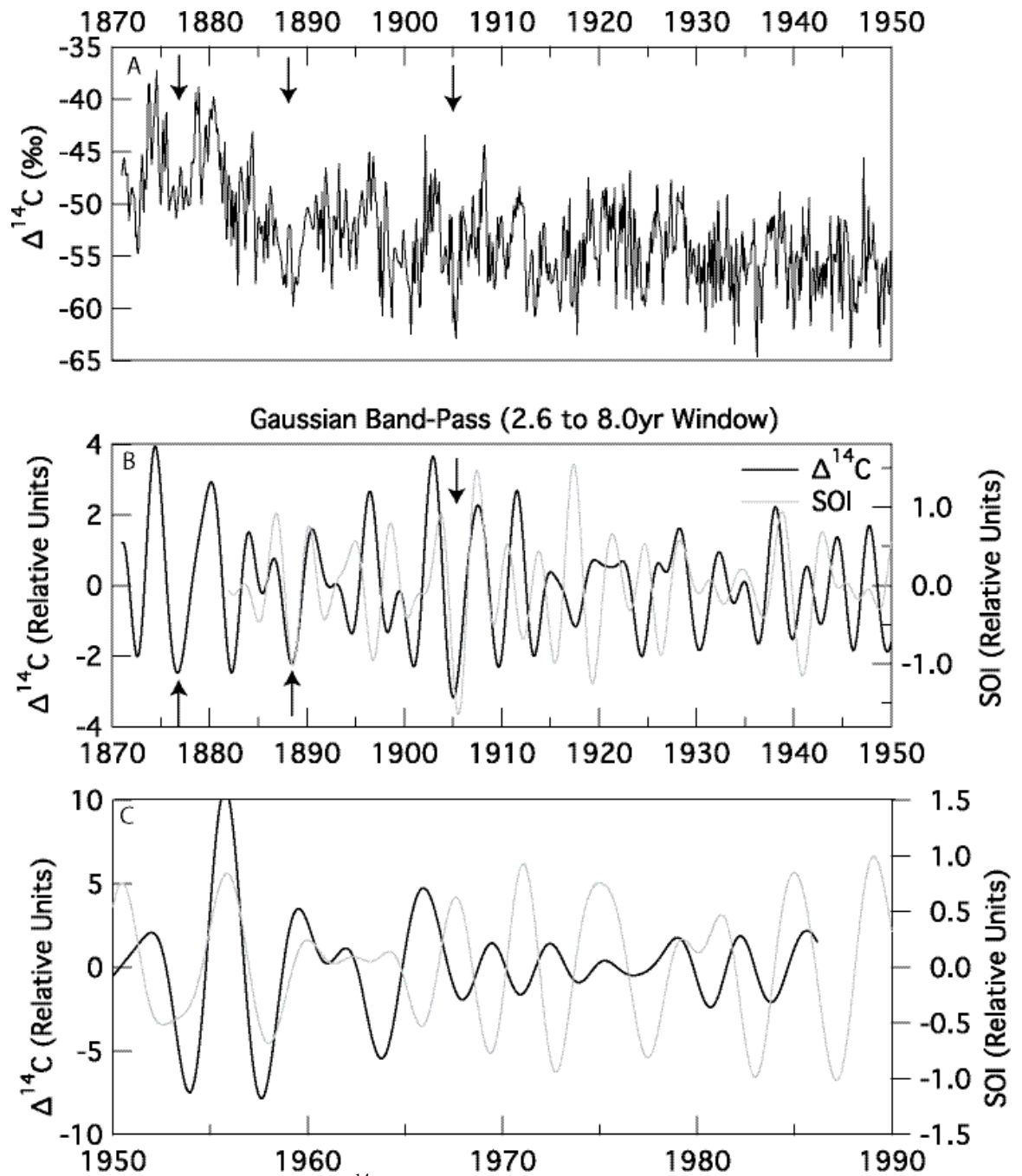


Figure 7. A. Prebomb Langkai coral $\Delta^{14}\text{C}$. B. Gaussian Band-Pass filter (2.6 to 8 yr. window) of Langkai coral $\Delta^{14}\text{C}$ and Southern Oscillation Index Langkai coral $\Delta^{14}\text{C}$ pre-bomb era. C. Gaussian Band-Pass filter (2.6 to 8 yr. window) of Langkai coral $\Delta^{14}\text{C}$ and Southern Oscillation Index Langkai coral $\Delta^{14}\text{C}$ post-bomb era. Arrows indicate selected El Niño events.